Hybrid lattice Boltzmann model for binary fluid mixtures

A. Tiribocchi,[1,2,*] N. Stella,[1,†] G. Gonnella,[1,2,‡] and A. Lamura[3,§]
[1]*Dipartimento di Fisica, Università di Bari, Via Amendola 173, 70126 Bari, Italy*
[2]*INFN, Sezione di Bari, Via Amendola 173, 70126 Bari, Italy*
[3]*Istituto Applicazioni Calcolo, CNR, Via Amendola 122/D, 70126 Bari, Italy*
(Received 26 January 2009; revised manuscript received 18 May 2009; published 7 August 2009)

A hybrid lattice Boltzmann method (LBM) for binary mixtures based on the free-energy approach is proposed. Nonideal terms of the pressure tensor are included as a body force in the LBM kinetic equations, used to simulate the continuity and Navier-Stokes equations. The convection-diffusion equation is studied by finite-difference methods. Differential operators are discretized in order to reduce the magnitude of spurious velocities. The algorithm has been shown to be stable and reproducing the correct equilibrium behavior in simple test configurations and to be Galilean invariant. Spurious velocities can be reduced by approximately an order of magnitude with respect to standard discretization procedure.

DOI: 10.1103/PhysRevE.80.026701 PACS number(s): 47.11.−j, 64.75.−g

I. INTRODUCTION

In recent years lattice Boltzmann methods (LBM) [1] have been widely used to study multiphase fluids [2]. Examples of applications are the analysis of growth regimes in phase separation of binary mixtures [3] or the study of backflow effects in liquid crystal behavior [4]. The LBM approach is well suited for dealing with complex geometries or for parallel implementations [1]. Moreover, in the free-energy approach [5], the mesoscale properties of the fluid (interface structures, coupling with local order parameters, etc.) can be straightforwardly inserted in the LBM numerical scheme and taken under control. Due to the relevance of the method, it is worth to further develop LBM algorithms in order to improve numerical stability and accuracy, also by optimizing the use of computer resources.

LBM dynamics is defined in terms of kinetic equations for a set of populations f_i representing, at each lattice site and time, the density of particles moving in one of the allowed directions of a given lattice. The sum over the directions i of f_i is the local density of the fluid while the first momentum is related to the local fluid momentum. In one approach a forcing term is included in the kinetic equations representing the interactions between the components of the mixture [6]. Differently, the free-energy method was originally developed by fixing the second moment of the populations in terms of the pressure tensor of the fluid mixture [7]. It has been applied to complex fluids in Refs. [8–10].

In this paper we consider an approach similar to the one of Ref. [11] where a free-energy dependent term is added as a body force in the kinetic equations. This approach traces back to the work of Guo *et al.* [12] where a comparison with different methods to introduce the force is reported. With respect to the algorithm of Ref. [7], this allows a better control of the continuum limit still keeping all the advantages of the free-energy method. In Ref. [11] a lattice Boltzmann equation is considered for each component. Here we consider a "hybrid" algorithm where LBM is used to simulate Navier-Stokes equations while finite-difference methods are implemented to simulate the convection-diffusion equation. Such hybrid codes have been used for complex fluids [13], liquid crystals [14], and thermal flows [15]. This allows to reduce in a relevant way the amount of required memory in systems with multicomponent order parameters or in simulations of three-dimensional systems.

A typical undesired effect due to discretization is the appearing of unphysical flow close to the interfaces. This flow, often known as spurious velocities, can severely affect the quality of LBM simulations. In this work we discretize the differential operators by a procedure optimized for reducing the magnitude of spurious velocities, following the so-called "stencil" method applied in Ref. [16] to a multiphase one-component fluid. Here we will see that this method allows to reduce spurious velocities of about an order of magnitude.

The paper is organized as follows. In the next section the LBM algorithm proposed is described and details on the numerical implementation is given. In Sec. III results of simulations of test configurations are shown. We will see how spurious velocities around curved interfaces can be reduced applying a more general stencil to discretize derivatives. We will also discuss the convection of a drop under a constant force acting for a finite time interval. Then some conclusions will follow in Sec. IV.

II. MODEL

The equilibrium properties of the fluid mixture can be described by a free energy

$$\mathcal{F} = \int d\mathbf{r}\left[nT \ln n + \frac{a}{2}\varphi^2 + \frac{b}{4}\varphi^4 + \frac{\kappa}{2}(\nabla\varphi)^2 \right], \qquad (1)$$

where T is the temperature, n is the total density of the mixture, and φ is the scalar order parameter representing the concentration difference between the two components of the mixture. The term depending on n gives rise to the ideal gas

*adriano.tiribocchi@ba.infn.it
†nicolastella1@gmail.com
‡gonnella@ba.infn.it
§a.lamura@ba.iac.cnr.it

pressure $p^i=nT$ which does not affect the phase behavior. The terms in φ in the free-energy density $f(n,\varphi,T)$ correspond to the typical expression of Ginzburg-Landau free energy used in studies of phase separation [17]. The terms in the free energy can be distinguished in two parts: the polynomial terms describe the bulk properties of the mixture and the gradient term is related to the interfacial ones.

In the bulk terms the parameter b is always positive to ensure stability while the parameter a can distinguish a disordered ($a>0$) and an ordered ($a<0$) mixture, in which the two components coexist with equilibrium values $\pm\varphi_{eq}$ where $\varphi_{eq}=\sqrt{\frac{-a}{b}}$ [18]. The equilibrium profile between the two coexisting bulk components is

$$\varphi(x)=\varphi_{eq}\tanh\left(\frac{2x}{\xi}\right) \tag{2}$$

with interface width

$$\xi=2\sqrt{\frac{2\kappa}{-a}} \tag{3}$$

and surface tension

$$\sigma=\frac{2}{3}\sqrt{\frac{2a^2\kappa}{b}}. \tag{4}$$

The thermodynamic functions can be obtained from the free energy (1) by differentiation. The chemical-potential difference between the two components is given by

$$\mu=\frac{\delta\mathcal{F}}{\delta\varphi}=a\varphi+b\varphi^3-\kappa\nabla^2\varphi. \tag{5}$$

The pressure $P_{\alpha\beta}$ is a tensor since interfaces in the fluid can exert nonisotropic forces [19]. The diagonal part p_0 can be obtained from Eq. (1) as

$$\begin{aligned}p_0&=n\frac{\delta\mathcal{F}}{\delta n}+\varphi\frac{\delta\mathcal{F}}{\delta\varphi}-f(n,\varphi,T)\\&=p^i+\frac{a}{2}\varphi^2+\frac{3b}{4}\varphi^4-\kappa\varphi(\nabla^2\varphi)-\frac{\kappa}{2}(\nabla\varphi)^2.\end{aligned} \tag{6}$$

For a fluid with concentration gradients $P_{\alpha\beta}$ has to verify the general equilibrium condition $\partial_\alpha P_{\alpha\beta}=0$ [20]. A suitable choice for the pressure tensor is

$$P_{\alpha\beta}=p_0\delta_{\alpha\beta}+\kappa\partial_\alpha\varphi\partial_\beta\varphi. \tag{7}$$

The hydrodynamic equations of fluids follow from the conservation laws for mass and momentum. For binary mixtures at constant temperature the evolution of density, velocity, and concentration fields is described by the continuity, the Navier-Stokes and the convection-diffusion equations [21], respectively,

$$\partial_t n+\partial_\alpha(nu_\alpha)=0, \tag{8}$$

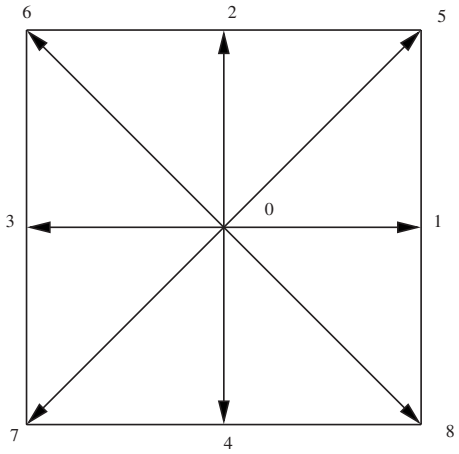

FIG. 1. Cell of the $D2Q9$ lattice used in the present study.

$$\begin{aligned}\partial_t(nu_\beta)+\partial_\alpha(nu_\alpha u_\beta)&=-\partial_\alpha P_{\alpha\beta}\\&+\partial_\alpha\left\{\eta\left(\partial_\alpha u_\beta+\partial_\beta u_\alpha-\frac{2\delta_{\alpha\beta}}{d}\partial_\gamma u_\gamma\right)+\zeta\delta_{\alpha\beta}\partial_\gamma u_\gamma\right\}\\&=-\partial_\beta(p^i)-\varphi\partial_\beta\mu+\partial_\alpha\left\{\eta\left(\partial_\alpha u_\beta+\partial_\beta u_\alpha-\frac{2\delta_{\alpha\beta}}{d}\partial_\gamma u_\gamma\right)\right.\\&\left.+\zeta\delta_{\alpha\beta}\partial_\gamma u_\gamma\right\},\end{aligned} \tag{9}$$

$$\partial_t\varphi+\partial_\alpha(\varphi u_\alpha)=\Gamma\nabla^2\mu, \tag{10}$$

where η and ζ are the shear and the bulk viscosities, Γ is the mobility coefficient, and d is the dimensionality of the system.

Equations (8)–(10) can be solved numerically. We use a mixed approach that consists of a finite-difference scheme for solving Eq. (10) and of a LBM approach with forcing term for Eqs. (8) and (9). This has the advantage that the amount of required memory can be decreased so that larger systems can be simulated. In our case of study, for a two-dimensional model on a square lattice with nine velocities ($D2Q9$), this method allows to reduce the required memory of $\sim$27%. Actually, the convection-diffusion equation could have also been solved on a $D2Q5$ lattice [22] and in this case the reduction in memory would have been of $\sim$17%. Moreover, the spurious terms in the continuum equations found in previous formulations based on a free energy [7] can be avoided.

A. Lattice Boltzmann scheme with forcing term

To solve Eqs. (8) and (9) we use a Lattice Boltzmann scheme on a lattice of size $L_x\times L_y$ in which each site is connected to nearest and next-to-nearest neighbors. This is one of the simplest geometries which reproduce correctly the Navier-Stokes equations in continuum limit and is shown in Fig. 1. Horizontal and vertical links have length Δx and diagonal links $\sqrt{2}\Delta x$. On each site $\mathbf{r}$ nine lattice velocity vectors $\mathbf{e}_i$ are defined. They have modulus $|\mathbf{e}_i|=\frac{\Delta x}{\Delta t_{LB}}\equiv c$, being Δt_{LB} the time step, for $i=1$, 2, 3, 4, and modulus $|\mathbf{e}_i|=\sqrt{2}c$ for

$i=5, 6, 7, 8$. Moreover, the zero velocity vector $\mathbf{e}_0=\mathbf{0}$ is defined. A set of distribution function $\{f_i(\mathbf{r},t)\}$ is defined on each lattice site $\mathbf{r}$ at each time t.

In the LB scheme for simple fluids [1] the distribution functions evolve during the time step Δt_{LB} according to a single relaxation-time Boltzmann equation [23]

$$f_i(\mathbf{r}+\mathbf{e}_i\Delta t_{LB},t+\Delta t_{LB})-f_i(\mathbf{r},t)=-\frac{\Delta t_{LB}}{\tau}[f_i(\mathbf{r},t)-f_i^{eq}(\mathbf{r},t)], \tag{11}$$

where τ is a relaxation parameter and $f_i^{eq}(\mathbf{r},t)$ are the local equilibrium distribution functions. The total density n and the fluid momentum $n\mathbf{u}$ are defined by the following relations

$$n=\sum_i f_i, \quad n\mathbf{u}=\sum_i f_i\mathbf{e}_i, \tag{12}$$

where $\mathbf{u}$ is the fluid velocity. The form of f_i^{eq} must be chosen so that the mass and momentum are locally conserved in each collision step, therefore the following relations must be satisfied:

$$\sum_i (f_i^{eq}-f_i)=0 \Rightarrow \sum_i f_i^{eq}=n, \tag{13}$$

$$\sum_i (f_i^{eq}-f_i)\mathbf{e}_i=0 \Rightarrow \sum_i f_i^{eq}\mathbf{e}_i=n\mathbf{u}. \tag{14}$$

Moreover, the f_i^{eq}'s need to have some symmetries so that the Navier-Stokes equations are reproduced in the continuum limit. A convenient choice for the local equilibrium distribution functions of an ideal fluid in the case of a $D2Q9$ model is given by a second-order expansion in the fluid velocity $\mathbf{u}$ of the Mawwell-Boltzmann distribution [24]

$$f_i^{eq}(\mathbf{r},t)=\omega_i n\left[1+\frac{\mathbf{e}_i\cdot\mathbf{u}}{c_s^2}+\frac{\mathbf{uu}:(\mathbf{e}_i\mathbf{e}_i-c_s^2\mathbf{I})}{2c_s^4}\right], \tag{15}$$

where $c_s=c/\sqrt{3}$ is the sound speed in this model, $\mathbf{I}$ is the unitary matrix and a suitable choice for the coefficients ω_i is $\omega_0=4/9$, $\omega_i=1/9$ for $i=1-4$, $\omega_i=1/36$ for $i=5-8$. This form is such that

$$\sum_i f_i^{eq}e_{i\alpha}e_{i\beta}=nc_s^2\delta_{\alpha\beta}+nu_\alpha u_\beta. \tag{16}$$

In order to simulate Eq. (9) where a nonideal pressure tensor $P_{\alpha\beta}$ appears, we adopt a LB model with a forcing term following a derivation similar to that of Ref. [12]. In the case of Ref. [12] the model was used to study forced simple fluids while we address the case of a binary mixture with interaction and interface contributions. The evolution equation of the distribution functions becomes

$$f_i(\mathbf{r}+\mathbf{e}_i\Delta t_{LB},t+\Delta t_{LB})-f_i(\mathbf{r},t)$$
$$=-\frac{\Delta t_{LB}}{\tau}[f_i(\mathbf{r},t)-f_i^{eq}(\mathbf{r},t)]+\Delta t_{LB}F_i, \tag{17}$$

where F_i is the forcing term to be properly determined. The equilibrium distribution functions (15) are not changed except for the formal substitution $\mathbf{u}\rightarrow\mathbf{u}^*$, where $\mathbf{u}^*$ is given by

$$n\mathbf{u}^*=\sum_i f_i\mathbf{e}_i+\frac{1}{2}\mathbf{F}\Delta t_{LB}, \tag{18}$$

$\mathbf{F}$ being the force density acting on the fluid and $\mathbf{u}^*$ the physical velocity. The expression of $\mathbf{F}$ for our case will be given later. The forcing term F_i can be expressed as a power series at the second order in the lattice velocity [25]

$$F_i=\omega_i\left[A+\frac{\mathbf{B}\cdot\mathbf{e}_i}{c_s^2}+\frac{\mathbf{C}:(\mathbf{e}_i\mathbf{e}_i-c_s^2\mathbf{I})}{2c_s^4}\right], \tag{19}$$

where A, $\mathbf{B}$, and $\mathbf{C}$ are functions of $\mathbf{F}$. The moments of the force verify the following relations

$$\sum_i F_i=A, \quad \sum_i F_i\mathbf{e}_i=\mathbf{B}, \quad \sum_i F_i\mathbf{e}_i\mathbf{e}_i=c_s^2A\mathbf{I}+\frac{1}{2}[\mathbf{C}+\mathbf{C}^T], \tag{20}$$

and have to be consistent with the hydrodynamic equations.

The continuum limit is obtained by using a Chapman-Enskog expansion in the Knudsen number ϵ,

$$f_i=f_i^{(0)}+\epsilon f_i^{(1)}+\epsilon^2 f_i^{(2)}+\cdots, \tag{21}$$

$$\partial_t=\epsilon\partial_{t_1}+\epsilon^2\partial_{t_2}, \tag{22}$$

$$\partial_{\mathbf{r}}=\epsilon\partial_{\mathbf{r}_1}, \tag{23}$$

$$\mathbf{F}=\epsilon\mathbf{F}_1, \quad A=\epsilon A_1, \quad \mathbf{B}=\epsilon\mathbf{B}_1, \quad \mathbf{C}=\epsilon\mathbf{C}_1. \tag{24}$$

We note that the force term is of first order in ϵ [26]. The continuity and the Navier-Stokes equations are recovered in the following form:

$$\partial_t(nu_\beta^*)+\partial_\alpha(nu_\alpha^*u_\beta^*)=-\partial_\beta(nc_s^2)+F_\beta+\partial_\alpha\{\eta(\partial_\alpha u_\beta^*+\partial_\beta u_\alpha^*)\} \tag{25}$$

in terms of the velocity $\mathbf{u}^*$ when the following expressions for the terms A, $\mathbf{B}$, $\mathbf{C}$:

$$A=0, \quad \mathbf{B}=\left(1-\frac{\Delta t_{LB}}{2\tau}\right)\mathbf{F}, \quad \mathbf{C}=\left(1-\frac{\Delta t_{LB}}{2\tau}\right)(\mathbf{u}^*\mathbf{F}+\mathbf{F}\mathbf{u}^*) \tag{26}$$

are used. The continuum Eqs. (8) and (25) can be also obtained by a Taylor expansion method. We remark that no spurious terms are present in the continuum equations except for a term of order u^{*3} which is neglected in Eq. (25). Such approximation is correct as far as $u^{*2}\ll c_s^2$ when the expansion (15) is valid [1]. In the present formulation the second moment of the equilibrium distribution function (16) does not need to be modified to include the effects of the pressure tensor as in previous models based on a free energy [7]. It is straightforward to show that the momentum defined in Eq. (18) corresponds to an average between the pre- and postcollisional values of the velocity $\mathbf{u}$ which is the correct way to calculate it when a forcing term is introduced [6,26]. It is this value that appears in the continuum equations and is measured in simulations. As in the case of standard LBM [1], the

present model is characterized by the fact that $\zeta=\frac{2}{d}\eta$ with shear viscosity

$$\eta = nc_s^2\Delta t_{LB}\left(\frac{\tau}{\Delta t_{LB}}-\frac{1}{2}\right). \tag{27}$$

In order to recover Eq. (9) we have to require that

$$\mathbf{F} = \nabla(nc_s^2 - p^i) - \varphi\nabla\mu = -\varphi\nabla\mu. \tag{28}$$

The last equality comes from the fact the term nc_s^2 corresponds in LBM to the ideal gas pressure p^i [1]. Finally, the forcing term in Eq. (17) has the form

$$F_i = \left(1-\frac{\Delta t_{LB}}{2\tau}\right)\omega_i\left[\frac{\mathbf{e}_i-\mathbf{u}^*}{c_s^2}+\frac{\mathbf{e}_i\cdot\mathbf{u}^*}{c_s^4}\mathbf{e}_i\right]\cdot\mathbf{F} \tag{29}$$

with $\mathbf{u}^*$ given by Eq. (18).

B. Numerical calculation of the forcing term

The derivatives of the order parameter in the forcing term (28) are calculated using a finite-difference scheme. In particular, we have adopted a stencil representation of finite-difference operators in the more general way to ensure higher isotropy [16], which is known to reduce spurious velocities [27,28]. The schemes for the x derivative and the Laplacian operators are, respectively,

$$\partial_{Dx} = \frac{1}{\Delta x}\begin{bmatrix} -M & 0 & M \\ -N & 0 & N \\ -M & 0 & M \end{bmatrix}, \tag{30}$$

$$\nabla_D^2 = \frac{1}{\Delta x^2}\begin{bmatrix} R & Q & R \\ Q & -4(Q+R) & Q \\ R & Q & R \end{bmatrix}, \tag{31}$$

with $2N+4M=1$ and $Q+2R=1$ to guarantee consistency between the continuous and discrete derivatives [16]. The subscript D in the symbols of derivatives denotes the discrete operator. In these schemes the central entry is referred to the lattice point where the derivative is computed, and the other entries are referred to the eight neighbor lattice sites. The discrete derivatives of the order parameter φ are computed by summing the values in the site and in the eight neighbors with the weights in the matrices (30) and (31). The y derivative is computed by transposing the matrix (30). The choice of the free parameters N and Q is made in such a way that the spurious velocities are minimized (see next section). We will refer to this case as the optimal choice (OC). The values $N=1/2$, $M=0$, $Q=1$, and $R=0$ correspond to the standard central difference scheme denoted as SC. We will compare SC and OC in the following.

C. Scheme for the convection-diffusion equation

The convection-diffusion Eq. (10) is solved by using a finite-difference scheme. The function $\varphi(\mathbf{r},t)$ is defined on the nodes of the same lattice used for the LB scheme. The time is discretized in time steps Δt_{FD} with time values $t^n=n\Delta t_{FD}$, $n=1,2,3,\ldots$. The relationship connecting the two time steps is $\Delta t_{LB}=m\Delta t_{FD}$, being m an integer. We denote any discretized function at time t^n on a node (x_i,y_j) $(i=1,2,\ldots,L_x; j=1,2,\ldots,L_y)$ of the lattice by $g(x_i,y_j,t^n)=g_{ij}^n$. At each time step we update $\varphi^n\rightarrow\varphi^{n+1}$ using Eq. (10) in two successive partial steps [29]. This allows to have a better numerical stability. In the first step we implement the convective term using an explicit Euler algorithm [30]

$$\varphi^{n+1/2} = \varphi^n - \Delta t_{FD}(\varphi^n\partial_\alpha u_\alpha^{*n} + u_\alpha^{*n}\partial_\alpha\varphi^n) \tag{32}$$

where the velocity $\mathbf{u}^*$ comes from the solution of the LB equation. Note that the term $\partial_\alpha u_\alpha^{*n}$ has not been neglected since the fluid is not exactly incompressible. Indeed, the Navier-Stokes Eq. (25) coming from the LBM contains some compressibility terms which can be anyway kept very small requiring that $u^{*2}\ll c_s^2$ [1]. The derivatives in Eq. (32) are discretized as follows:

$$\partial_{Dx}u_x^*|_{ij}^n = \frac{u_{x,(i+1)j}^{*n}-u_{x,(i-1)j}^{*n}}{2\Delta x}, \tag{33}$$

$$\partial_{Dx}\varphi|_{ij}^n = \frac{\varphi_{ij}^n-\varphi_{(i-1)j}^n}{\Delta x} \quad \text{if} \quad u_{x,ij}^{*n}>0, \tag{34}$$

$$\partial_{Dx}\varphi|_{ij}^n = \frac{\varphi_{(i+1)j}^n-\varphi_{ij}^n}{\Delta x} \quad \text{if} \quad u_{x,ij}^{*n}<0, \tag{35}$$

and analogously for the y components.

The diffusive part of Eq. (10) is implemented in the second update step using an explicit Euler algorithm as

$$\varphi^{n+1} = \varphi^{n+1/2} + \Delta t_{FD}\Gamma[a\nabla^2\varphi^{n+1/2} + b\nabla^2 f^n - \kappa\nabla^2(\nabla^2\varphi^{n+1/2})], \tag{36}$$

where $f^n=(\varphi^n)^3$ and the operator ∇^2 is discretized using the form given in Eq. (31) with the standard choice $Q=1$ and $R=0$. Other choices using a more general stencil for discretizing ∇^2 are possible though we checked that they did not provide any relevant difference.

III. RESULTS AND DISCUSSION

We considered several test cases in order to validate our model. We used the values $\Delta x=\Delta t_{LB}=\Delta t_{FD}=1$. In the free energy we adopted the parameters $-a=b=10^{-3}$, $\kappa=-3a$ corresponding to an equilibrium interface of width $\xi\simeq 5\Delta x$. The mobility Γ was set to 5 and the relaxation time $\tau/\Delta t_{LB}$ was 1 unless differently stated.

We first examined the relaxation to equilibrium of a planar sharp interface on a lattice of size $L_x=L_y=64$ varying τ in the SC case. In all the cases the system correctly relaxes to the expected profile (2). One example is reported in Fig. 2. In the case of a planar interface the fluid velocities u^* decay to negligible values as it should be at equilibrium when $\Delta\mu=0$ and $\partial_\alpha P_{\alpha\beta}=0$.

We then studied a circular drop as a test for a case with interfaces not aligned with the lattice links. A drop with sharp interface of diameter $64\Delta x$ was placed at the center of a lattice of size $L_x=L_y=128$ and let equilibrate in the SC

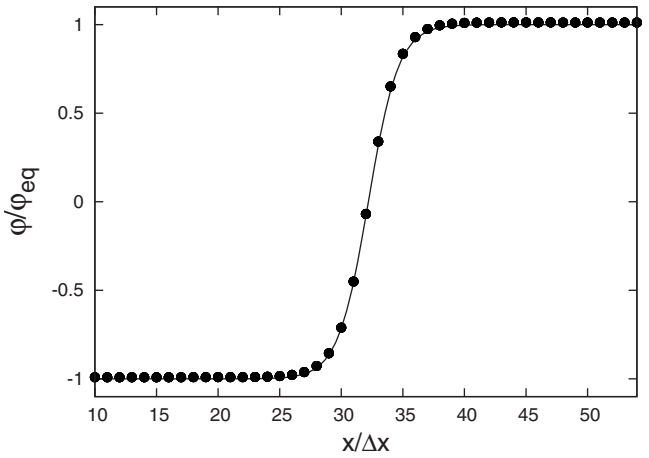

FIG. 2. Equilibrium profile of a planar interface on a lattice of size $L_x=L_y=64$ in the SC case. The continuous line is the analytical result (2) and data points are the results of simulations.

case. Interfaces relax to the expected profile without deforming the drop but spurious velocities appear as it can be seen in the upper panel of Fig. 3 in the case with $\tau/\Delta t_{LB}=5$. We then used the OC scheme to verify whether spurious velocities could be reduced by using a more isotropic structure for the discrete spatial derivatives in the forcing term (28). We scanned several values of N and Q in order to reduce the maximum value of the velocity $|u^*_{\max}|$ on the whole lattice. The optimal values are summarized in the Table I. It is interesting to note that there is a couple of values $N=0.3$ and $Q=2.5$ which occurs more frequently. We verified that this choice is also effective in reducing spurious velocities even for the other values of τ. For this choice of N and Q the maximum velocities differ only by a small percentage from the tabled values.

Velocities can be greatly reduced with respect to the SC case as it can be visually observed in the lower panel of Fig. 3.

We also tried to get an analytical estimate of the optimal values of N and Q in the following way. At equilibrium it holds that $\partial_\alpha P_{\alpha\beta}=\varphi\partial_\beta\mu=(a\varphi+3b\varphi^3)\partial_\beta\varphi-k\varphi\partial_\beta(\nabla^2\varphi)=0$. This expression depends on the first- and third-order derivatives. By using the stencils (30) and (31) we get for the discretized operators the expressions

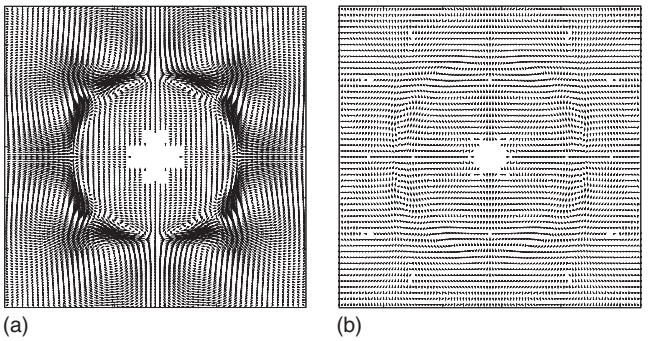

FIG. 3. Velocity patterns (the same scale is used in both the panels) at equilibrium when $\tau/\Delta t_{LB}=5$ in the SC case (upper panel) and in the OC case (lower panel). Empty spaces are due to negligible values of velocity. In both the cases the system has size $L_x=L_y=128$.

TABLE I. Optimal values of N and Q for different values of τ and the corresponding values of the maximum spurious velocity $|u^*_{\max}|$.

$\tau/\Delta t_{LB}$	N	Q	$\lvert u^*_{\max}\rvert/c_s$
0.6	0.3	3	0.0001753
0.8	0.3	2.5	0.0000603
1	0.3	2.5	0.0000365
1.2	0.3	2.5	0.0000267
5	0.3	2.5	0.0000088
10	0.3	2	0.0000062

$$\partial_{Dx}=\partial_x+\frac{1}{6}(\Delta x)^2\partial_x^3+\frac{1-2N}{2}(\Delta x)^2\partial_x\partial_y^2+\cdots \tag{37}$$

and

$$\nabla_D^2=\nabla^2+\frac{1}{12}(\Delta x)^2(\partial_x^4+\partial_y^4)+\frac{1-Q}{2}(\Delta x)^2\partial_x^2\partial_y^3+\cdots, \tag{38}$$

so that

$$\partial_{Dx}(\nabla_D^2)=\partial_x(\nabla^2)+\frac{1}{4}(\Delta x)^2\partial_x^5+\left[\frac{1}{6}+\frac{1-2N}{2}+\frac{1-Q}{2}\right]\times(\Delta x)^2\partial_x^3\partial_y^2+\left[\frac{1}{12}+\frac{1-2N}{2}\right](\Delta x)^2\partial_x\partial_y^4+\cdots. \tag{39}$$

By imposing that the error terms in the third-order derivative depending on N and Q vanish, we get $N=7/12\simeq 0.6$ and $Q=7/6\simeq 1.2$. However, this estimate does not correspond to the optimal results of Table I. This is due to the fact that these optimal values were found by considering the full dynamical problem with the whole set of equations where we minimized the spurious velocities. In the estimate after Eq. (40) the coupling with the velocity field was not taken into account so that there is no *a priori* reason to expect the same optimal values for N and Q.

A comparison of the spurious velocities in the SC and OC cases is shown in Fig. 4. By using the optimal choice OC the spurious velocities can be reduced by a factor approximately 10 with respect to the standard case SC over the whole range of τ values. The stencil forms (30) and (31) were also applied to the model of Ref. [7] for nonideal fluids finding a comparable reduction in the magnitude of spurious velocities with respect to the standard case [16].

We then studied the motion of an equilibrated drop of diameter $64\Delta x$ in a lattice of size $L_x=256$, $L_y=128$ under the effect of an external constant force that acts up to the time $t/\Delta t_{LB}=500$ and is then switched off. The additional force $\mathbf{G}=n(g_x,0)\Delta x^2/\Delta t_{LB}$ acts on the total density. g_x is in the range $[10^{-5},5\times10^{-5}]$ and the OC scheme is used. The overall system is set in motion rightward with increasing velocity

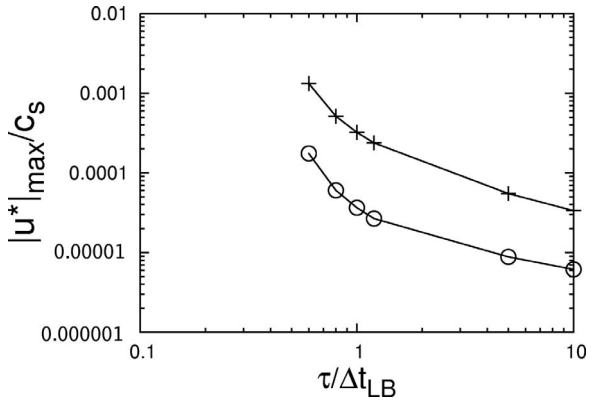

FIG. 4. Maximum spurious velocities as a function of τ in the SC case (+) and in the OC case (○).

until the force **G** is on, then it moves with constant speed. The choice of g_x is such that the final velocity is much smaller than the speed of sound c_s. The aim was to check whether the system is Galilean invariant and the drop is correctly convected by the flow. We monitored the shape of the drop and measured its center-of-mass velocity $\mathbf{v}_{CM}$. This is defined as the average velocity of the center of mass whose position is

$$\mathbf{r}_{CM}(t) = \frac{\Sigma_{ij}\varphi_{ij}\mathbf{r}_{ij}(t)}{\Sigma_{ij}\varphi_{ij}}, \tag{40}$$

where the sum is over the lattice nodes $\mathbf{r}_{ij}$ inside the drop. This velocity represents the convection velocity and is compared with the fluid velocity $\mathbf{v}_f(t)=\mathbf{u}^*[\mathbf{r}_{CM}(t)]$ at the center of mass given directly by the LBM. In Fig. 5 the comparison between the velocities $\mathbf{v}_{CM}$ and $\mathbf{v}_f$ along the x direction is shown in the case with $g_x=3\times10^{-5}$. It is evident that the two coincide indicating that the drop is correctly advected by the fluid. Moreover, its shape is not altered by motion as it can be seen in Fig. 6 where some configurations of the system at

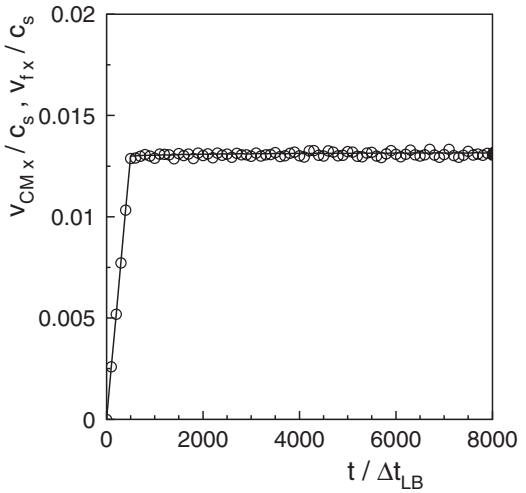

FIG. 5. Velocities of the center of mass of the drop v_{CMx} (○) and of the fluid v_{fx} (—) at the center of mass along the x direction as a function of time. The external force acts until the time $t/\Delta t_{LB}=500$.

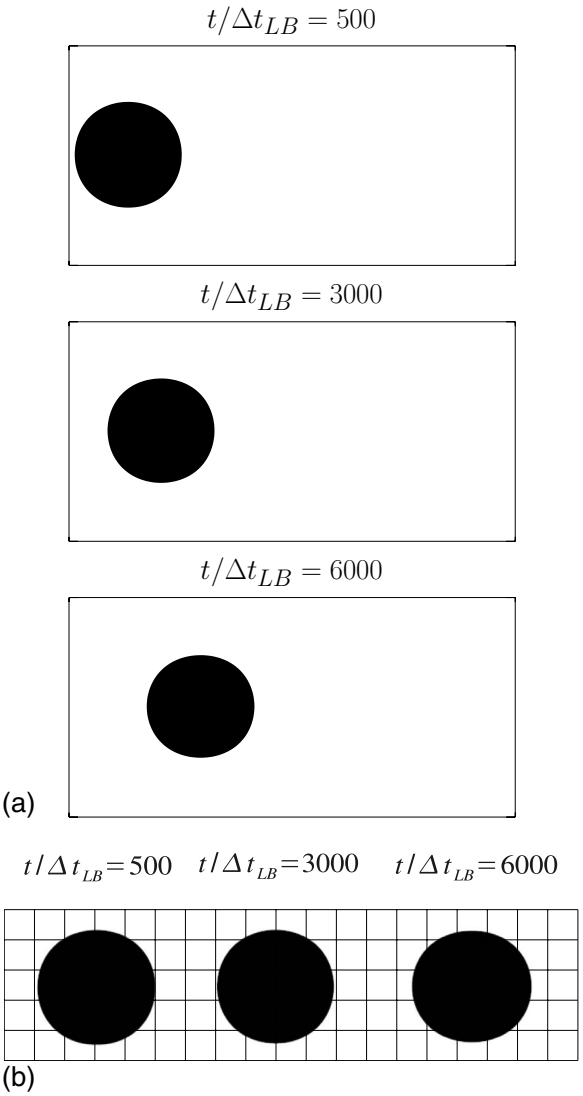

FIG. 6. Configurations of the advected drop at consecutive times. The system has size $L_x=256$, $L_y=128$. In the lower panel the drop, extracted from the system, is shown on an underlying mesh to better appreciate its shape.

different times are presented. Moreover, the drop is shown to make clear that it does not change in shape with time. We measured the ratio of the horizontal and vertical diameters finding that it stays almost constant with a deviation less than 3% from the value 1. If the advection velocity is higher, the drop will be slightly deformed being stretched along the x direction. This effect becomes negligible when increasing the surface tension (4) via the parameter κ.

IV. CONCLUSIONS

In this paper we have considered a lattice Boltzmann method for binary mixtures with thermodynamics fixed by a free-energy functional. We used a mixed method, with continuity and Navier-Stokes equations simulated by LBM, and convection-diffusion equation by finite-difference schemes. Differently than in previous free-energy LBM formulations [7], the interaction part in the pressure tensor is not intro-

duced by fixing the second moment of the LBM populations but by introducing a forcing term in the lattice equation. This approach is suggested by a microscopic picture and allows to obtain a continuum limit without spurious terms. On the other hand, the mixed or hybrid approach allows a reduction in the required memory and this can be relevant in performing large-scale simulations.

In order to reduce spurious velocities, differential operators have been discretized by generalizing the usual lattice representations. Free parameters appear and their optimal values have been fixed by requiring that the maximum value of spurious velocities at equilibrium is minimized.

We considered simple test situations, flat interfaces and single drops showing that the correct equilibrium profiles are reproduced. We found that spurious velocities are reduced of about an order of magnitude when a more general stencil is applied to the derivatives in the forcing term of the LBM equations. We did not found any relevant difference by applying this procedure to the differential operators appearing in the convection-diffusion equation. We also checked that our method is stable in phase-separation studies, even if we have not reported the results of these simulations in this work. Finally, we checked the effective Galilean invariance of the system by advecting for some time interval by a constant force a configuration with one drop and then letting the system to evolve without forcing. For the cases considered, we did not observe relevant drop deformations, the drop being correctly advected by the surrounding fluid. In conclusion, we hope that this development of the free-energy LBM can be useful in future simulations of binary mixtures and complex fluids.

[1] R. Benzi, S. Succi, and M. Vergassola, Phys. Rep. **222**, 145 (1992); S. Chen and G. D. Doolen, Annu. Rev. Fluid Mech. **30**, 329 (1998); S. Succi, *The Lattice Boltzmann Equation for Fluid Dynamics and Beyond* (Clarendon Press, Oxford, 2001).

[2] B. Dünweg and A. J. C. Ladd, Adv. Polym. Sci. **221**, 89 (2009).

[3] V. M. Kendon, J.-C. Desplat, P. Bladon, and M. E. Cates, Phys. Rev. Lett. **83**, 576 (1999).

[4] C. Denniston, E. Orlandini, and J. M. Yeomans, Phys. Rev. E **63**, 056702 (2001).

[5] J. M. Yeomans, Annu. Rev. Comput. Phys. **VII**, 61 (1999).

[6] X. Shan and H. Chen, Phys. Rev. E **49**, 2941 (1994).

[7] E. Orlandini, M. R. Swift, and J. M. Yeomans, Europhys. Lett. **32**, 463 (1995); M. R. Swift, E. Orlandini, W. R. Osborn, and J. M. Yeomans, Phys. Rev. E **54**, 5041 (1996).

[8] G. Gonnella, E. Orlandini, and J. M. Yeomans, Phys. Rev. Lett. **78**, 1695 (1997).

[9] A. Lamura, G. Gonnella, and J. M. Yeomans, Europhys. Lett. **45**, 314 (1999).

[10] M. E. Cates, S. M. Fielding, D. Marenduzzo, E. Orlandini, and J. M. Yeomans, Phys. Rev. Lett. **101**, 068102 (2008).

[11] Q. Li and A. J. Wagner, Phys. Rev. E **76**, 036701 (2007).

[12] Z. Guo, C. Zheng, and B. Shi, Phys. Rev. E **65**, 046308 (2002).

[13] A. G. Xu, G. Gonnella, and A. Lamura, Physica A **362**, 42 (2006).

[14] D. Marenduzzo, E. Orlandini, M. E. Cates, and J. M. Yeomans, Phys. Rev. E **76**, 031921 (2007).

[15] P. Lallemand and L. S. Luo, Int. J. Mod. Phys. B **17**, 41 (2003); F. Dubois and P. Lallemand, e-print arXiv:0811.0599.

[16] C. M. Pooley and K. Furtado, Phys. Rev. E **77**, 046702 (2008).

[17] A. J. Bray, Adv. Phys. **43**, 357 (1994).

[18] J. S. Rowlinson and B. Widom, *Molecular Theory of Capillarity* (Clarendon Press, Oxford, 1982).

[19] A. J. M. Yang, P. D. Fleming, and J. H. Gibbs, J. Chem. Phys. **64**, 3732 (1976).

[20] R. Evans, Adv. Phys. **28**, 143 (1979).

[21] S. R. De Groot and P. Mazur, *Non-equilibrium Thermodynamics* (Dover Publications, New York, 1984).

[22] I. Rasin, S. Succi, and W. Miller, J. Comput. Phys. **206**, 453 (2005).

[23] P. L. Bhatnagar, E. P. Gross, and M. Krook, Phys. Rev. **94**, 511 (1954).

[24] Y. Qian, D. d'Humieres, and P. Lallemand, Europhys. Lett. **17**, 479 (1992).

[25] A. J. C. Ladd and R. Verberg, J. Stat. Phys. **104**, 1191 (2001).

[26] J. M. Buick and C. A. Greated, Phys. Rev. E **61**, 5307 (2000).

[27] X. Shan, Phys. Rev. E **73**, 047701 (2006).

[28] M. Sbragaglia, R. Benzi, L. Biferale, S. Succi, K. Sugiyama, and F. Toschi, Phys. Rev. E **75**, 026702 (2007).

[29] S. M. Fielding, Phys. Rev. E **77**, 021504 (2008).

[30] J. C. Strikwerda, *Finite Difference Schemes and Partial Differential Equations* (Chapman and Hall, New York, 1989).